

MODELLING OF UAV FLIGHT DYNAMICS USING PERCEPTRON ARTIFICIAL NEURAL NETWORKS

JERZY MANEROWSKI
DARIUSZ RYKACZEWSKI

Air Force Institute of Technology, Warsaw

e-mail: jerzy.manerowski@itwl.pl; dariusz.rykaczewski@itwl.pl

The methodology of modelling flight dynamics of UAV using perceptron artificial neural networks has been presented. The modelling is based on experimental data recorded during flight characteristic and performance tests of UAVs that is a part of a set to give training to anti-aircraft artillery. The artificial neural network structure in quasi-static and dynamic flights have been given. The accuracy indexes also have been given.

Key words: Unmanned Aerial Vehicle (UAV), flight mechanics, mathematical modelling, artificial neural networks

1. Introduction

Identification of flight dynamical models of unmanned aerial vehicles (UAVs) is taken up by many research institutions. Computer methods of the identification are used supported by experimental data (Manerowski and Rykaczewski, 2003). As a new branch in science and technology artificial neural networks (ANNs) have appeared (Borowczyk *et al.*, 1998; Hazarika, 1998; Rutkowska *et al.*, 1999). One of the most important characteristics of ANNs is parallel processing of information by all neurons. In many cases, the parallel processing is possible on-line. One of interesting applications of ANNs is identification in flight control (Borowczyk *et al.*, 1998; Hazarika, 1998; Horn and Calise, 1998; James, 1997; Lonnblad *et al.*, 1992), which is the subject of research. Distinctly different from linear equations, non-linear relationships are much complicated and analytical solutions are impossible. Instead, approximate ANN mathematical models are used, which are adapted during a

learning process (Lonnblad *et al.*, 1992). The identification problem is to construct a model and to describe its parameters. From many possible solutions, a multi-layer perceptron neural network has been chosen.

To work out a mathematical model of a UAV, experimental data has been used (Fig. 1) and examined during tests at the Air Force Institute of Technology (AFIT). Experimental flight data was recorded by a flight recorder. Recorded data were: G -forces, angle velocities, speed and height of the flight, aileron displacement, rotational speed of the propeller and UAV's GPS coordinates. These experimental data were used then for the learning process. In the learning process, back propagation algorithms were used, which defined the strategy of weights selection in a multi-layer ANN (Manerowski, 1999). As a result, the structure of the ANN was defined, i.e. the number of layers and neurons as well as the structure of input and output parameters in full flight dynamics of the UAV.

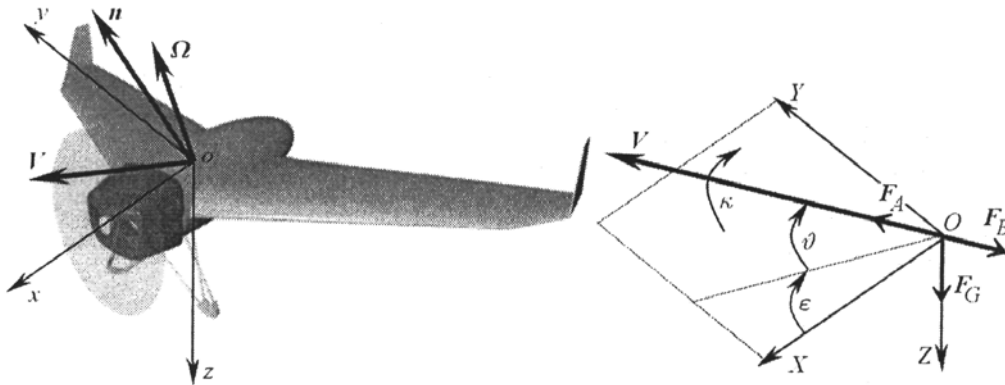


Fig. 1. Flying object UAV

2. Problem formulation

To formulate a mathematical model of a UAV, classic laws of flight mechanics were used (Bociak and Gruszecki, 1999; Manerowski, 2001). On the basis of these laws, equations of motion were determined considering the flying object as a rigid solid. Generally, equations of motion can be presented as

$$\dot{V}_{V\Omega} = \mathbf{B}^{-1}(\mathbf{F}_A + \mathbf{F}_B + \mathbf{F}_G + \dots) \quad (2.1)$$

where

- B** – inertia matrix
F_A – force vector and moment of inertia
F_B – vector of inertia forces
F_G – vector of *G*-forces.

On the basis of analysis by Manerowski (2001), his equation of motion were incorporated to formulate the mathematical model of the UAV. In the mentioned equations, the linear vector of acceleration $\dot{\mathbf{V}}$ and the vector of angular velocities $\dot{\varepsilon}$ (deflection) and $\dot{\vartheta}$ (slope) are generally linked by the formula

$$\dot{\mathbf{V}}_{\vartheta\varepsilon} = \mathbf{E}_V \mathbf{E}_t \mathbf{E}^\top \mathbf{n} \quad (2.2)$$

where $\dot{\mathbf{V}}_{\vartheta\varepsilon}$ is the vector of motion parameters (Fig. 1). It consists of components

$$\dot{\mathbf{V}}_{\vartheta\varepsilon} = [\dot{V}, \dot{\vartheta}, \dot{\varepsilon}]^\top \quad (2.3)$$

\mathbf{E}_V is a matrix that has the following form

$$\mathbf{E}_V = g \left[1, \frac{1}{V}, \frac{1}{V \cos \vartheta} \right] \quad (2.4)$$

while \mathbf{E}_t – depends on the angles ε and ϑ (Fig. 1)

$$\mathbf{E}_t = \begin{bmatrix} \cos \vartheta \cos \varepsilon & \cos \vartheta \sin \varepsilon & -\sin \vartheta \\ -\sin \vartheta \cos \varepsilon & -\sin \vartheta \sin \varepsilon & -\cos \vartheta \\ -\sin \varepsilon & \cos \varepsilon & 0 \end{bmatrix} \quad (2.5)$$

$\mathbf{n} = [n_x, n_y, n_z]^\top$ is a vector of *G*-loads in the *xyz* co-ordinate system (Fig. 1). Its components are longitudinal *G*-load (n_x), side *G*-load (n_y) and gravity load (n_z).

\mathbf{E} is a matrix of transformation expressed in terms of Euler's angles Φ , Θ and Ψ (Manerowski, 2001) (Fig. 2)

$$\mathbf{E}_t = \begin{bmatrix} \cos \Psi \cos \Theta & \sin \Psi \cos \Theta & -\sin \Theta \\ e_{21} & e_{22} & \cos \Theta \sin \Phi \\ e_{31} & e_{32} & \cos \Theta \cos \Phi \end{bmatrix} \quad (2.6)$$

where

$$\begin{aligned} e_{21} &= \cos \Psi \sin \Theta \sin \Phi - \sin \Psi \cos \Phi \\ e_{22} &= \sin \Psi \sin \Theta \sin \Phi + \cos \Psi \cos \Phi \\ e_{31} &= \cos \Psi \sin \Theta \cos \Phi + \sin \Psi \sin \Phi \\ e_{32} &= \sin \Psi \sin \Theta \cos \Phi - \cos \Psi \sin \Phi \end{aligned}$$

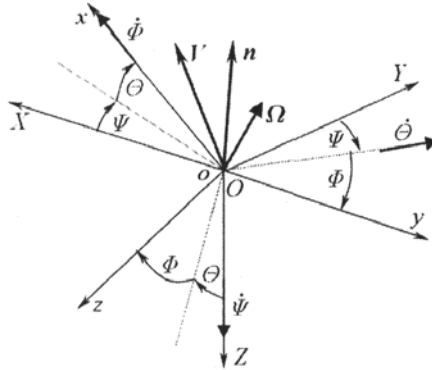


Fig. 2. Euler's angles (Φ, Θ, Ψ) between two coordinate systems (xyz - co-ordinate related to object, $OXYZ$ - co-ordinate related to ellipsoid surface)

Changes of the velocity V , slope angle ϑ and deflection angle ε with respect to time and position of the flying object and with respect to the given co-ordinate (Fig. 1) can be presented in a functional way depending on the G -loads vector \mathbf{n} and angular velocity of bank $\dot{\kappa}$

$$\dot{V}_{\vartheta\varepsilon} = f(\mathbf{n}, \dot{\kappa}, \dots) \quad (2.7)$$

Moreover, \mathbf{n} and $\dot{\kappa}$ depend on the velocity V , aileron displacement δ_h , differential aileron displacement $\Delta\delta_h$ and derivatives of these parameters. The idea of the paper is to formulate G -loads vector \mathbf{n} and bank angular velocity $\dot{\kappa}$, in relation to flight and control parameters. As a result, equations of motion were determined, (2.8), whose the solution was found by methods of numerical integration, while the G -loads and the bank angle κ were generated by perceptron neural networks

$$\begin{bmatrix} \dot{V}_s \\ \dot{\vartheta} \\ \dot{\varepsilon} \end{bmatrix} = \begin{bmatrix} g & 0 & 0 \\ 0 & \frac{g}{V_s} & 0 \\ 0 & 0 & \frac{g}{V_s \cos \vartheta} \end{bmatrix} \begin{bmatrix} 1 & 0 & 0 \\ 0 & -\sin \kappa & -\cos \kappa \\ 0 & \cos \kappa & -\sin \kappa \end{bmatrix} \left(\begin{bmatrix} n_x \\ -n_y \\ -n_z \end{bmatrix} + \begin{bmatrix} -\sin \vartheta \\ \cos \vartheta \sin \kappa \\ \cos \vartheta \cos \kappa \end{bmatrix} \right) \quad (2.8)$$

To get prejudiced in favour of computational results, it is worth to mark that good results are obtained when using a separate ANN to generate a single parameter of G -loads and bank angle κ . The G -loads are modelled separately for quasi-static and dynamic flights (quasi-static component - st sign, dynamic component - dyn sign) according to

$$n_\alpha = n_{\alpha st} + n_{\alpha dyn} \quad \alpha = x, y, z \quad (2.9)$$

3. ANN model

An artificial neural network (ANN) is a mathematical model that allows formulating output signals \mathbf{n} , in that case G -loads, in relation to input signals \mathbf{p} , whereas, basically, these should be normalised signals (Fig. 3).



Fig. 3. A mathematical scheme of a neural model of a flying object; \mathbf{p} – vector of input signal $[V_i, \delta_{hi}, \Delta\delta_{hi}, \dots]$, \mathbf{p}' – vector of normalised input signal, \mathbf{n}' – vector of normalised output signal, \mathbf{n} – G -loads vector $[n_{xi}, n_{yi}, n_{zi}]$, \mathbf{A} , \mathbf{B} – matrices of signal transformation

3.1. Model in quasi-static flight

The structure of an ANN in a quasi-static flight with experimental data used is shown in Fig. 4. The input data are: velocity, aileron displacement and rotational velocity of the propeller at the i -th moment. The output data are G -loads at the i -th moment.

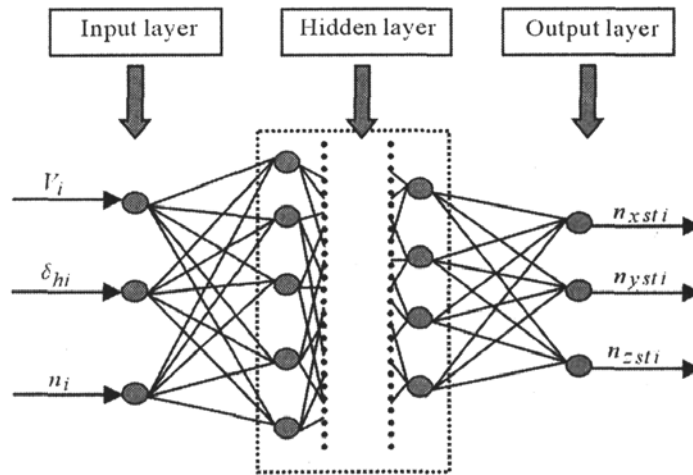


Fig. 4. The structure of an ANN in a quasi-static flight

3.2. Model in dynamic flight

The structure of an ANN in a dynamic flight is shown in Fig. 5. The output data at the i -th moment depend on quasi-static parameters at that

moment and depend on the input data at the previous moments: $i - 1$, $i - 2$, etc.

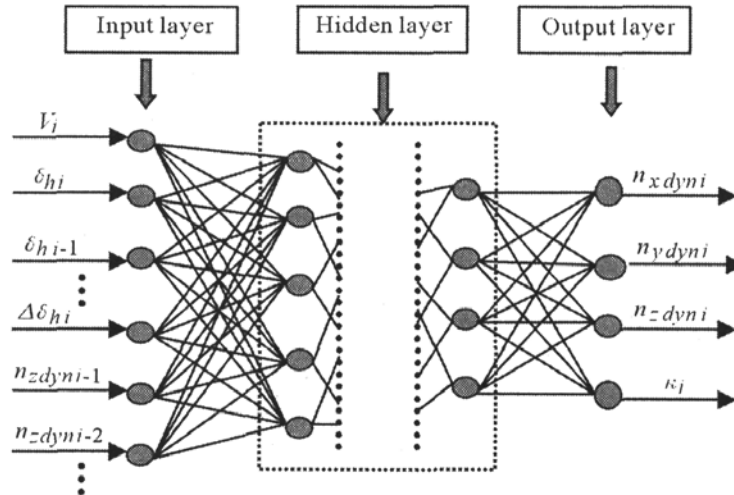


Fig. 5. The structure of an ANN in a dynamic flight

4. Results

Numerical computations were carried out based upon the ANN JETNET 2.0 software (Lonnblad *et al.*, 1992) using a back propagation algorithm. To learn the ANN, experimental data of a UAV were used. The computations were made for different structures of the ANN. Unfavourable results for an incorrect ANN structure are presented in Fig. 6 and Fig. 7, whereas favourable results (ANN worked correctly) in Fig. 8 and Fig. 9. As an example, G -loads generated by the ANN were presented below as a function of aileron displacement for selected velocities.

Positive and negative G -loads of the whole flight were generated by the ANN. Experimental data for learning process were prepared. After computations, the best results were taken by a separate ANN to generate a single output parameter, which meant separate modelling of the ANN for any G -loads. The generated gravity load n_z by the ANN is presented in Fig. 8.

A very interesting problem is to generate the dynamic component of the G -load taken from recorded loads. The recorded loads consist of two components: quasi-static and dynamic. Quasi-static components are G -loads at the

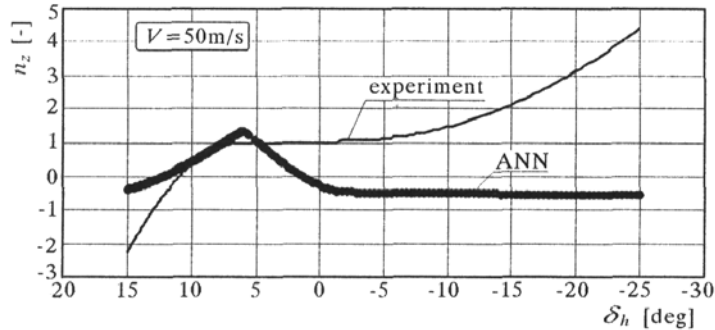


Fig. 6. Gravity load n_z generated by a $3 \times 4 \times 4 \times 3$ ANN (unfavourable case)

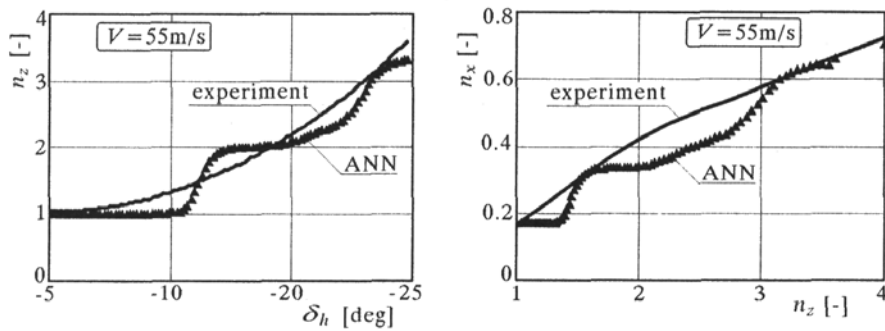


Fig. 7. G -loads generated by a $3 \times 4 \times 3$ ANN (unfavourable case)

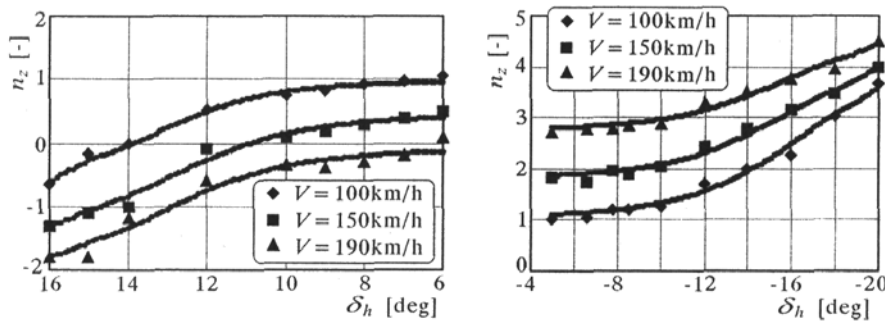


Fig. 8. Generated gravity load n_z by a separate ANN

i -th moment, depending on the input parameters ($V_i, \delta_{hi}, T_i, \dots$) and dynamic components depending on derivatives of these data. In accordance with that methodology, the dynamic component was taken as subtraction of the quasi-static component generated by the quasi-static ANN from the recorded parameters. Below the dynamic component is presented in relation to an im-

pulsive aileron displacement for a specified flight. It is worth to know that the accuracy during the learning process of the dynamic ANN depends on repeating of the process N . The number of repetitions N is one order higher than that in the quasi-static ANN. For a specific flight, the generated dynamic component of the gravity load is presented in Fig. 9 for an impulsive aileron displacement.

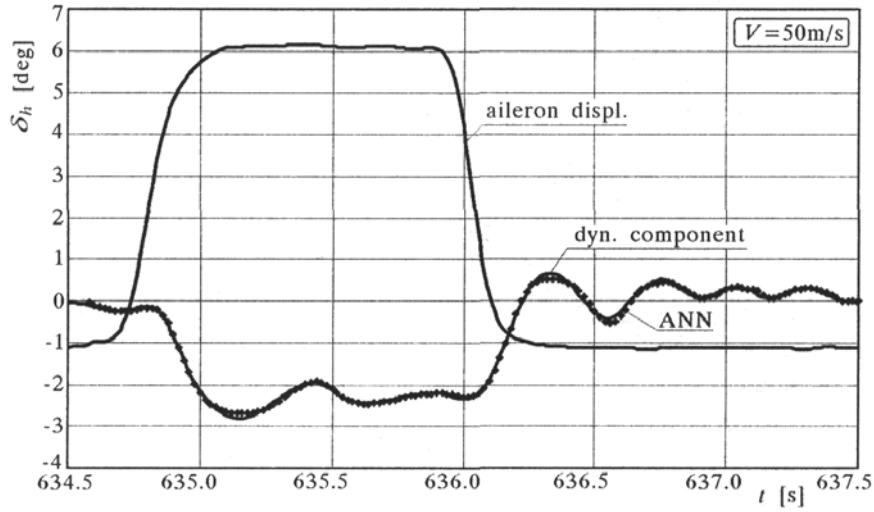


Fig. 9. Dynamic change of the gravity load in relation to aileron displacement

The evaluation of accuracy of the generated G -loads was made as follows:

- average sum of components taken from experimental recorded data (n_{ie}) and generated by the ANN (n_i) to the power of two

$$\chi_{mean}^2 = \frac{\chi^2}{N} \quad (4.1)$$

whereas

$$\chi^2 = \sum_{i=1}^N \chi_i^2 \quad \chi_i^2 = (n_{ie} - n_i)^T (n_{ie} - n_i) \quad (4.2)$$

- positive case l_p to meet the condition

$$(n_{ie} - n_i)^T (n_{ie} - n_i) < 0.01 \quad i = 1, 2, \dots, N \quad (4.3)$$

n_{ie} – experimental G -load at the moment i

n_i – G -load generated by the ANN at the moment i .

The influence of the ANN structure and its parameters such as the learning factor η and momentum α (Osowski, 2000) on the accuracy indexes is given below.

Table 1

α/η	ANN structure			Positive cases l_p [%]	Index $\chi^2_{mean} \cdot 10^{-2}$	
	input neurones	hidden neurones	output neurones			
0.8/0.4	3	4	-	1	13	23.329
0.7/0.3					22	0.731
0.6/0.2					58	0.282
0.5/0.1					99	0.017
0.1/0.05					98	0.056
0.8/0.4	8	4	-	1	18	19.338
0.7/0.3					44	7.161
0.6/0.2					45	0.799
0.5/0.1					97	0.703
0.1/0.05					95	0.121
0.8/0.4	3	4	4	1	65	0.863
0.7/0.3					34	7.543
0.6/0.2					98	0.766
0.5/0.1					100	0.103
0.1/0.05					100	0.084
0.8/0.4	8	4	4	1	24	43.223
0.7/0.3					46	17.544
0.6/0.2					35	33.654
0.5/0.1					95	0.487
0.1/0.05					99	0.077
0.8/0.4	8	6	6	1	17	13.049
0.7/0.3					27	26.556
0.6/0.2					44	5.834
0.5/0.1					99	0.096
0.1/0.05					99	0.042
0.8/0.4	8	4	4	1	50	7.657
0.7/0.3					40	10.923
0.6/0.2					88	0.282
0.5/0.1					99	0.027
0.1/0.05					99	0.083

5. Summary

To compare the results taken from experimental data and generated by the ANN it is worth to mention that the mathematical model of a UAV using the ANN is satisfactory. It can be concluded that the perceptron neural network can be used for UAV modelling and testing its performance. That ANN model consists of:

- eight neurones in the input layer
- four neurones in separate two hidden layers
- one neurone in the output layer.

The most important thing is to realize that good accuracy in generating flight data, in quasi-static and dynamic flights, requires separate ANNs to generate single parameters. Therefore, to work out a mathematical model of the UAV, it was necessary to build the same number of ANNs as output parameters. Moreover, in the dynamic model of the UAV, the number of repetitions N in the learning process is one order higher than the corresponding number in a quasi-static ANN model.

References

1. BOCIEK S., GRUSZECKI J., 1999, *Układy sterowania automatycznego samolotem*, Oficyna Wydawnicza Politechniki Rzeszowskiej, Rzeszów
2. BOROWCZYK H., LEWITOWICZ J., LINDSTEDT P., 1998, The neural diagnostic method and a complex system of diagnosing airframe and power plant, *ICAS-98*
3. HAZARIKA N., 1998, An inverse design procedure for airfoils using artificial neural networks, *ICAS-98*
4. HORN J., CALISE A., 1998, Flight envelope limiting systems using neural network, *AIAA Atmospheric Flight Mechanics Conference*, Boston
5. JAMES E., 1997, Some application of artificial neural networks in modelling of non-linear aerodynamics and flight dynamics, *AIAA*, Paper 97-0338
6. LONNBLAD L., PETERSON C., ROGNVALDSSON T., 1992, Pattern recognition in high energy physics with artificial neural networks – JETNET 2, *Computer Physics Communications*, **70**, Sweden
7. MANEROWSKI J., 1999, *Identyfikacja modeli dynamiki ruchu sterowanych obiektów latających*, Wydawnictwo Naukowe ASKON, Warszawa

8. MANEROWSKI J., 2001, Modelowanie dynamiki lotu samolotu z wykorzystaniem sztucznych sieci neuronowych, *Prace Naukowe ITWL*, **13**, Warszawa
9. MANEROWSKI J., RYKACZEWSKI D., 2003, Modelowanie dynamiki lotu bezpilotowego statku latającego z zastosowaniem sztucznych sieci neuronowych, *Prace Naukowe ITWL*, **17**, Warszawa
10. MARQUES F., 1998, Identification of aircraft non-linear dynamics using Volterra series, *ICAS-98*
11. OSOWSKI S., 2000, *Sieci neuronowe do przetwarzania informacji*, Oficyna Wydawnicza Politechniki Warszawskiej, Warszawa
12. RUTKOWSKA D., PILIŃSKI M., RUTKOWSKI L., 1999, *Sieci neuronowe, algorytmy genetyczne i systemy rozmyte*, PWN, Warszawa

Identyfikacja modelu dynamiki lotu bezpilotowego statku powietrznego z wykorzystaniem perceptronowych sztucznych sieci neuronowych

Streszczenie

W artykule przedstawiono metodologię modelowania dynamiki lotu bezpilotowego statku powietrznego z wykorzystaniem perceptronowych sztucznych sieci neuronowych. Modelowanie oparto na wynikach eksperymentu uzyskanych podczas badań własności lotnych i osiągnięć bezpilotowego statku powietrznego wchodzącego w zestaw celów powietrznych do szkolenia wojsk OPL. Podano, w zagadnieniu quasi-ustalonym oraz dynamicznym, strukturę sieci neuronowej odwzorowującej własności lotne takiego obiektu oraz wskaźniki oceny dokładności.

Manuscript received July 27, 2004, accepted for print November 30, 2004